Journal of Spacecraft and Rockets
Vol. 44, No. 1, January–February 2007

Hypersonic Missile Performance and Sensitivity Analysis

Con J. Doolan*
University of Adelaide, South Australia 5005, Australia

DOI: 10.2514/1.23160

The performance of a conceptual, missile-class, hypersonic vehicle was modeled using a 2-degree-of-freedom dynamics model. The vehicle was assumed to be air launched, accelerated to a Mach number of 3 using a solid propellant rocket, and subsequently propelled using a dual-mode scramjet engine to cruise at Mach numbers between 4 and 9. Modeling results show that fuel storage capacity and dynamic pressure have a significant effect on vehicle range and average speed. A perturbation analysis was also performed that ranked the sensitivity of missile range to small changes in 14 design parameters. The kinetic energy efficiency (total pressure loss) of the scramjet has the highest effect on performance at high cruise Mach numbers (6.7–9), followed by structural mass, combustion efficiency, and aerodynamics parameters. At low cruise Mach numbers (4–6.7), structural concerns dominate performance, followed by the aerodynamics and scramjet operating parameters.

Nomenclature

A_{ref} = aerodynamic reference area, m^2
C_C = nondimensional heat of combustion per unit mass of air
C_D = drag coefficient
C_{Do} = zero-lift drag coefficient
C_F = nondimensional fuel enthalpy at the injector manifold per unit mass of air
C_L = lift coefficient
C_{PF} = fuel specific heat, J/kg/K
D = drag, N
f = fuel-air ratio
f_{bs} = booster structure mass fraction
$f_{s,\mathrm{wpn}}$ = weapon structure mass fraction
g = acceleration due to gravity, m/s^2
g_0 = acceleration due to gravity at sea level, m/s^2
h = altitude, m
h_0 = release altitude, m
h_∞ = freestream enthalpy, J/kg
I_{sa} = airbreathing engine specific impulse, s
I_{sb} = booster specific impulse, s
k = aerodynamic constant
L = lift, N
L_g = centrifugal lift, N
M_b = boost Mach number
M_0 = release Mach number
M_∞ = freestream Mach number
m = mass, kg
m_i = initial missile mass, kg
m_{payload} = payload mass, kg
n = aerodynamic exponent
Q_{HV} = fuel heating value, J/kg
q_∞ = dynamic pressure, Pa
R_b = range for baseline condition, m
R_E = radius of the Earth, 6378 km
T = thrust, N
T_F = fuel temperature, K
t_b = burn time of booster, s
u_0 = vehicle velocity at start of cruise, m/s
V = vehicle velocity, m/s, volume, m^3
V_∞ = freestream velocity, m/s
W_{final} = vehicle weight at end of cruise, N
W_{initial} = vehicle weight at start of cruise, N
x = range, m
x_0 = release range, m
γ = flight path angle, rad, ratio of specific heats
η_C = combustion efficiency
η_{KE} = kinetic energy efficiency
η_v = volumetric efficiency
κ_∞ = nondimensional specific flight kinetic energy
ρ = density, kg/m^3
ρ_f = liquid fuel density, kg/m^3
ρ_i = initial vehicle density, kg/m^3
ρ_p = propellant density, kg/m^3
Υ_p = propellant volume fraction

I. Introduction

HYPERSONIC missiles are an attractive technology for air-launched strike weapons, due to their long range, rapid response time and high impact velocity. Hypersonic missiles are also the most likely and useful near-term application of supersonic combustion ramjet (scramjet) propulsion systems. It is of great importance that the performance of proposed or conceptual hypersonic missile systems be understood early in the design process, to ensure that practical systems are selected for further development. More generally, recent flight testing of hypersonic vehicles [1,2] has renewed interest in understanding performance and design issues associated with hypersonic vehicles.

Hypersonic vehicles are commonly referred to as integrated, that is, vehicle subsystems are highly coupled so that it is impossible to modify one without significantly affecting the performance of other subsystems and the entire vehicle. However, it is still of interest to designers to understand what subsystem affects overall vehicle performance the most, when taking into account the interactional effects with other major subsystems. For example, it is unclear if aerodynamics, scramjet flow losses, or structural mass fraction dominate performance or if subsystem sensitivity changes with flight conditions. By understanding what design parameter the performance is most sensitive to, hypersonic system designers and researchers can systematically focus their efforts on the most relevant technology for a given application.

To design hypersonic systems such as missiles of practical size with useful range, airbreathing propulsion systems using liquid hydrocarbon fuels are necessary. Typically, scramjets are used to provide thrust [3] in conceptual hypersonic missile systems. These devices use an inlet device to diffuse the oncoming air to a lower, but

Presented as Paper 222 at the 44th AIAA Aerospace Sciences Meeting and Exhibit, Reno Nevada, 9–12 January 2006; received 12 February 2006; revision received 29 June 2006; accepted for publication 14 July 2006.

*Lecturer, School of Mechanical Engineering; con.doolan@mecheng.adelaide.edu.au. Member AIAA.

still supersonic, Mach number. Fuel is then injected into this supersonic airstream where it mixes and combusts, raising the energy of the flow before exhausting through a throatless nozzle to the atmosphere, generating thrust. The strength of the shock system in the inlet (and isolator, if present) is usually unaffected by the downstream processes in the combustion chamber. If high equivalence ratios and/or low flight Mach numbers are required (such as in an accelerative, low Mach number boost phase), the scramjet engine is capable of operating efficiently in a subsonic combustion ramjet mode, with a normal shock train in the isolator/inlet. This system is often called a dual-mode scramjet, and they are a popular choice for missile design studies as they allow efficient operation from Mach 3 to Mach 10 using hydrocarbon fuel [3].

One of the earliest documented hypersonic missile projects was the SCRAM (supersonic combustion ramjet missile) program, details of which were published by Billig in 1995 [4]. This project developed hypersonic missile configurations over the period 1962–1978 which included an axisymmetric, engine integrated design and a "pod-mounted" engine arrangement where scramjet engines were mounted around an ogive body. Both operated in two stages where a solid rocket booster launched the weapon system from the deck of a ship to a flight Mach number of 3.5–4. After booster separation, the scramjet engines ignited and accelerated the system to a high flight Mach number suitable for cruise. Special reactive fuels (boranes and aluminum alkyls) were developed for scramjet combustion and, using these fuels, various performance estimates were made. Billig [4] cites Mach 6.5 cruise at sea level and Mach 8.5 cruise at 30 km altitude, although it was recognized that material performance may not be capable of surviving in this aerothermodynamic environment. It was quoted that a 56.7–65.8 kg payload could be carried to ranges in excess of 740 km at cruise altitudes of 30 km. To intercept low altitude targets, the missile would fly at an optimum altitude and then dive to engage the target. Issues such as targeting, guidance, and control were either not investigated or were not published in the open literature.

After the SCRAM program, attention was focused on the dual-combustor ramjet or DCR. Fry [3] and Curran [5] provide excellent reviews of the development of this technology. The DCR is a dual-mode scramjet device where two combustors are used, an initial subsonic combustor operating fuel rich is used to supply a second supersonic combustor. The subsonic combustor is a combined flame holding and piloting technique that eliminates the need to use reactive fuel additives that are difficult to use in practice. Recently, the use of cavity-based fuel injector and flame stabilization techniques have become popular for use in hydrocarbon fueled dual-mode scramjets [6,7]. While there is a reasonable amount of experimental data for hydrocarbon fueled cavity-based combustors operating with a shock train upstream of the injector, there is little available for such a system operating in a supersonic combustion mode. Some recent numerical results by Kim et al. [8] for hydrogen fueled supersonic combustion with cavity-based injection illustrates the importance of total pressure loss and mixing efficiency on combustor performance.

The University of Maryland [9–12] has performed a series of hypersonic airbreathing missile design studies, concentrating on surface launched naval applications and waverider airframe geometries. Combustor modeling varies from a simple heat addition model to a more sophisticated chemical kinetics approach. These studies show that the performance of hydrocarbon fueled hypersonic missiles are sensitive to a range of design and thermodynamic parameters, especially the kinetics dominated ignition location. The high sensitivity of performance to ignition location is a strong argument in favor of incorporating an ignition device rather than relying on kinetically controlled ignition.

While these studies provide an invaluable insight into the performance of hypersonic missiles, they do not take into account the variation of lift-to-drag ratio (L/D) that occurs during cruise due to fuel consumption affecting vehicle weight. In addition, there is only a simplistic approach taken to incorporating mixing losses occurring within the combustor. Only the combustion efficiency is taken into account while it should be recognized that additional entropy gain due to fuel injection and mixing can significantly alter scramjet thrust levels [13–15].

For this study, a new hypersonic system performance model was developed that adds to the existing body of literature. This model integrates the equations of motion for the vehicle over the entire mission, rather than solving the unmodified Breguet range equation as is done in previous studies. Using the unmodified Breguet range equation in isolation does not take into account the significant effect of fuel consumption on aerodynamic trim in cruise [16]. Similarly, the airbreathing propulsion model used here takes into account combustor total pressure loss and combustion inefficiency, as it will be shown that these loss mechanisms have a significant effect on overall performance.

This paper will describe the performance model and use it to determine the range of two baseline hypersonic missile concepts. A sensitivity study will then be presented that illustrates the relative importance of each design characteristic for a cruise Mach number range of 4–9.

II. Performance Model

The operation of the hypersonic missile concept is assumed to occur in three phases. The first is solid rocket boost to a specified Mach number and dynamic pressure (altitude) from an air-launched initial condition. The dynamic pressure is specified as this is an important parameter in maintaining efficient combustion in dual-mode scramjet combustors. Once the boost phase is complete, the boost motor is discarded and the second phase begins. Here, a dual-mode scramjet propulsion system is ignited and the vehicle is accelerated in a ballistic, constant dynamic pressure climb to the specified cruise Mach number. The lift component during the second phase was not considered in order to simplify the analysis and to give conservative results. During the third phase (cruise), the vehicle is trimmed to maintain constant altitude and velocity, while remaining under scramjet propulsion.

A. Equations of Motion

It is assumed that a point-mass form of the equations of motion is adequate to model the performance of the hypersonic missile. Bilimoria and Schmidt [17] have derived a 3-degree-of-freedom, point-mass hypersonic vehicle dynamics model which includes the effects of altitude and spherical Earth effects. Here, this model is reduced to a 2-degree-of-freedom formulation by assuming that there is no vehicle side slip or roll so that the hypersonic missile is constrained to fly in a great-circle plane with the thrust aligned with the velocity vector. The system of equations is simplified further by neglecting the wind terms and the effects associated with the rotation of the Earth. Figure 1 describes the forces acting at the center of mass of the hypersonic missile and shows the alignment of thrust and velocity vectors. The inertial position of the vehicle center of mass is described by the curvilinear position along the Earth's surface (range) and altitude with respect to a fixed location on the Earth's surface E. The initial position of the missile at launch is an altitude h_0 directly above E so that $x_0 = 0$. The flight path angle is the angle the velocity vector makes with the local horizontal.

The point-mass vehicle equations of motion are [17,18],

$$\dot{V} = \frac{1}{m}(T - D - mg\sin\gamma) \tag{1}$$

$$\dot{\gamma} = \frac{1}{mV}(L_g\cos\gamma + L - mg\cos\gamma) \tag{2}$$

$$\dot{x} = V\frac{R_E}{R_E + h}\cos\gamma \approx V\cos\gamma \tag{3}$$

$$\dot{h} = V\sin\gamma \tag{4}$$

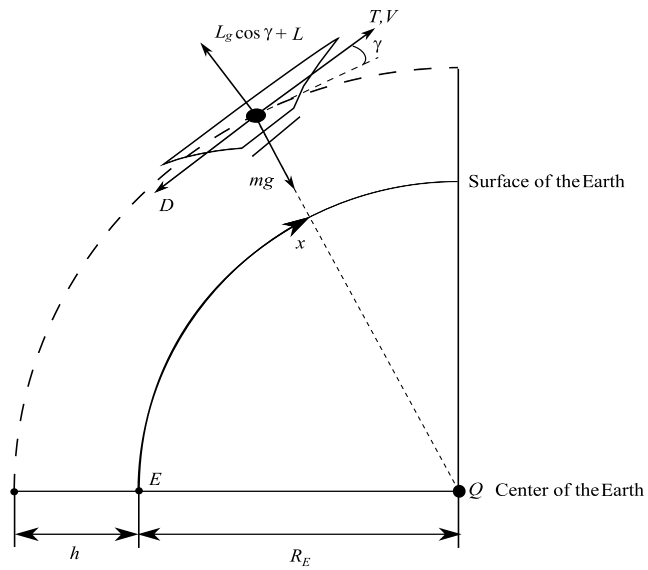

Fig. 1 Forces acting on the hypersonic missile.

The acceleration due to gravity is dependent on altitude,

$$g = g_0\left(\frac{R_E}{R_E + h}\right)^2 \tag{5}$$

The centrifugal term is defined as

$$L_g = \frac{mV^2}{R_E + h} \tag{6}$$

Differentiating Eqs. (3) and (4) and substituting into Eqs. (1) and (2) gives the point-mass equations of motion in the form used here,

$$m\ddot{x} = T\cos\gamma - D\cos\gamma - L\sin\gamma - L_g\cos\gamma\sin\gamma \tag{7}$$

$$m\ddot{h} = L_g\cos^2\gamma + L\cos\gamma - mg + T\sin\gamma - D\sin\gamma \tag{8}$$

Equation (7) is derived using the approximation shown in Eq. (3). If this approximation is not used, an additional acceleration term is included that couples $\dot{x}$ and $\dot{h}$. However, simulations including this additional term resulted in only small changes in the range performance (<0.1%), so the form shown in Eq. (7) is considered accurate for this study.

L, D, and T are determined through aerodynamic and propulsion models that are specific to the flight phase and propulsion technique. The solid rocket booster thrust is determined using an assumed specific impulse ($I_{sb} = 250$ s), propellant mass and burn time ($t_b = 25$ s). Hence, the mass fraction of the booster is fixed for each overall system mass and dynamic pressure chosen for the climb and cruise phases of the mission.

B. Airbreathing Propulsion

To model scramjet propulsion accurately, proper consideration of flow losses in the combustor must be given. Flow losses are caused by a number of factors that include viscous effects, shock waves, heat release, heat transfer, fuel/air mixing and chemical kinetics. While computational fluid dynamic models of ram/scramjet combustors provide detailed modeling of many aspects of these losses, they are computationally expensive and are unsuitable for a study such as the current one where many solution calls are required to solve for the vehicle performance. Here, an analytical formulation is used to model the specific impulse generated by a dual-mode scramjet.

Masuya et al. [15] show that ram/scramjet performance can be modeled using two parameters to represent combustor flow losses. These are η_C and η_{KE}. The combustion efficiency indicates how well combustion and heat release are achieved in the engine while the kinetic energy efficiency represents the loss in kinetic energy available to produce propulsive work. The kinetic energy efficiency is an alternative for total pressure loss ratio as total pressure is difficult to calculate in high enthalpy flows. Airbreathing specific impulse is calculated using the following relation [15]:

$$I_{sa} = \frac{V_\infty}{fg}\left\{\left[(1+f)\eta_{KE}\left(\frac{\eta_C C_C + C_F}{1+\kappa_\infty} + 1\right)\right] - 1\right\} \tag{9}$$

where

$$\kappa_\infty \equiv \frac{(\gamma_\infty - 1)M_\infty^2}{2} \tag{10}$$

The nondimensionalized fuel parameters C_C and C_F are calculated using

$$C_C = Q_{HV} f/h_\infty \tag{11}$$

$$C_F = C_{PF} T_F f/h_\infty \tag{12}$$

Jet A fuel at stoichiometric conditions is used for all simulations with $Q_{HV} = 43.4$ MJ/kg, $C_{PF} = 1181$ J/kg/K, $T_F = 300$ K, and $f = 0.0676$. Using these values, typical nondimensional fuel parameters are $C_C \approx 13.5$ and $C_F \approx 0.11$.

Masuya et al. [15] cite Curran et al. [19] who compiled available specific impulse data for ramjets and scramjets. For hydrocarbon fueled, subsonic combustion ramjets, it was found that available data was well correlated with $\eta_C = 1$ and $\eta_{KE} = 0.64$. For hydrogen fueled scramjets, a correlation of the available data yields $\eta_C = 0.7$ and $\eta_{KE} = 0.8$. In the absence of experimental data for Jet A fueled scramjet engines, the values $\eta_C = 0.7$ and $\eta_{KE} = 0.8$ are used.

Equation (9) can be compared with hydrocarbon fueled scramjet specific impulse predictions from the literature [11,16] and this is shown in Fig. 2. Figure 2 plots the specific impulse as calculated using Eq. (9) assuming an equivalence ratio of unity ($f = 0.0676$) assuming that Jet A has the same H/C molar ratio as cyclohexane) and a flight altitude of 30 km. The specific impulse is plotted using both "realistic" performance parameters ($\eta_C = 0.7$ and $\eta_{KE} = 0.8$) based on hydrogen scramjet tests and the most "optimistic" ($\eta_C = 1$ and $\eta_{KE} = 1$) which represents no flow losses. Specific impulse predictions from Starkey and Lewis [11] were obtained from quasi-one-dimensional calculations of a scramjet combustor flow field using Jet A fuel. The data chosen for comparison was for scramjets operating at altitudes and equivalence ratios close to those used to calculate the specific impulse from Eq. (9). Despite incorporating viscous losses, chemical kinetics, and a mixing efficiency, the

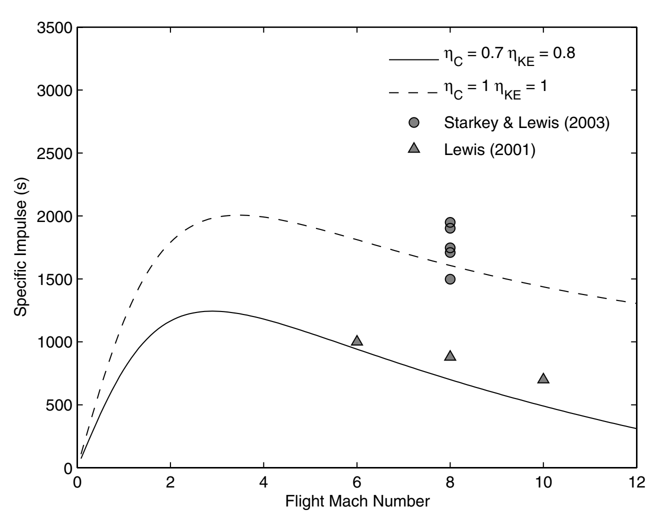

Fig. 2 Specific impulse for hydrocarbon fueled airbreathing propulsion systems ($f = 0.0676$, $h = 30$ km).

calculated specific impulses are close to the "optimistic" estimation (i.e., $\eta_C = 1$ and $\eta_{KE} = 1$). Better correlation is obtained with the "realistic" estimation (i.e., $\eta_C = 0.7$ and $\eta_{KE} = 0.8$) using the specific impulse calculations of Lewis [16]. Here, the specific impulse is calculated using a 50% thrust-power efficiency in line with the hydrogen fueled specific impulse estimations of Kerrebrock [20].

Therefore, the assumption that the hydrogen scramjet derived efficiencies can be used for Jet A in Eq. (9) appears reasonable.

C. Aerodynamics

The boost and climb phases of the flight are assumed to be ballistic. Therefore, no aerodynamic lift occurs during these phases of the flight and vertical force is provided by the propulsion system and to a lesser extent by the centrifugal force at high speeds. For the cruise phase of the flight, lift is set to the vehicle weight (corrected for the centrifugal component) and thrust is set to the drag. As discussed by Raymer [21] and Lewis [16], assuming a constant lift-to-drag ratio (L/D) is usually a poor assumption as the mass of the vehicle changes significantly due to the consumption of fuel. As vehicle mass is reduced, the reduction in lift must be accommodated by changing the angle of attack of the missile if it is to cruise at constant dynamic pressure and Mach number. Here, the drag is separated into two components, the zero-lift component (C_{Do}), and a component due to lift (kC_L^n) [16]. The lift-to-drag ratio is then

$$\frac{L}{D} = \frac{C_L}{C_{\mathrm{Do}} + kC_L^n} \tag{13}$$

where k and n are parameters that relate the induced drag to lift. Thus by calculating the lift requirement from the vehicle mass and speed, the drag penalty associated with this lift requirement can be determined. The required cruise thrust is equal to the cruise drag.

D. Airbreathing Constant Dynamic Pressure Climb

During airbreathing climb, the missile is set to zero angle of attack and is lifted by the action of the propulsion system. To provide relatively constant thermodynamic conditions to the propulsion system inlet, a constant dynamic pressure is specified throughout the climb and cruise phases of flight. To achieve this, the correct amount of thrust at each point during the climb needs to be determined.

By differentiating the definition of dynamic pressure with respect to time, the acceleration requirement to maintain constant dynamic pressure can be found,

$$\dot{V} = -\frac{q_\infty}{\rho_\infty^2}\frac{\mathrm{d}\rho}{\mathrm{d}h}\sin\gamma \tag{14}$$

Substituting Eq. (14) into Eq. (1) yields the thrust required to maintain a constant dynamic pressure climb at an angle γ with respect to the local horizontal,

$$T = mg\sin\gamma - m\frac{q_\infty}{\rho_\infty^2}\frac{\mathrm{d}\rho}{\mathrm{d}h}\sin\gamma + D \tag{15}$$

The term $\mathrm{d}\rho/\mathrm{d}h$ is calculated using the atmosphere model. For the current study, the 1976 U.S. standard atmosphere [22,23] is used. The differential is calculated using a second order central differencing technique.

E. Geometry

The calculation of missile performance is reliant on realistic estimates of the mass and volumes of various components of the missile. For analysis purposes, the initial mass of the missile is separated into the solid rocket booster and the weapon. Here the weapon consists of everything except the solid rocket booster (i.e., airbreathing propulsion system, liquid fuel, payload, and supporting structure including pumps, etc.). The performance of the missile is coupled with the structure and area available for aerodynamic force production. In the current study, this area is generalized into A_{ref}, a representative planform area. It is related to the volume using a η_v using $A_{\mathrm{ref}} = \eta_v V^{2/3}$. Determination of a suitable value of η_v is not straightforward. It is intricately linked to the structural layout of missile and aerodynamic surfaces. For waverider class hypersonic cruise vehicles, $\eta_v \approx 0.2$ [9]. The missile geometry is assumed to be constrained by ρ_i. Combined with m_i, a total missile volume can be calculated.

F. Numerical Solution Technique

The performance model is coded in Matlab 7. In each phase, the equations of motion are solved using the Matlab "stiff" ordinary differential equation (ODE) solver "ode15s."

Boost Mach number and dynamic pressure are specified by the user and the role of the booster is to insert the weapon at the appropriate altitude and speed to achieve this specification. Given the overall missile mass, the required booster mass to achieve the desired Mach number and dynamic pressure is determined by an iterative procedure. Here, f_{bs} and γ are varied in a nested Newton–Raphson technique until the desired conditions are met. A tolerance of 10^{-7} is used to determine convergence for all iterative procedures in the current study. Once f_{bs} has been determined, all other mass, area, and volume quantities can be determined for the remaining flight phases.

When the booster phase is complete, the initial conditions for the climb phase (i.e., mass, velocity, range, and altitude) are obtained from the last solution call of the boost phase. The mass is, however, modified as the boost motor is discarded to maximize performance. The climb angle is maintained at a constant 45 deg for simplicity. Again, an iterative technique is used to determine when the weapon achieves the cruise Mach number. This is done by varying the flight time in the climb phase in a progressive manner until actual and desired cruise Mach numbers vary by less than the specified tolerance. At all times, fuel mass is monitored and if more fuel is consumed in the climb phase than is available, the simulation aborts and the user is notified.

When the weapon achieves its specified cruise Mach number and there is fuel remaining, the cruise phase of the solution commences. The iterative procedure for the cruise phase is a progressive changing of the flight time until the fuel at the end of the cruise phase is within the numerical tolerance. Range of the missile is defined as the total distance it has traveled from air launch until all liquid fuel is consumed. Similarly, missile flight time is defined as the time between air launch and when all liquid fuel is consumed. Average missile speed is the missile range divided by the missile flight time.

Additional range can be calculated by assuming a glide phase where the missile glides to the target at an optimal aerodynamic setting. This range is not calculated as it is considered that the powered range is more representative of an operational weapon system.

III. Results

A. Baseline Concepts

The performance of two baseline hypersonic missile concepts was calculated using the model presented above. Parameters describing the missile concepts are listed in Table 1. All parameters are identical for each missile concept apart from the structural mass fraction of the weapon ($f_{s,\mathrm{wpn}}$), which varies from 0.6 to 0.5 in the two examples presented. The value $f_{s,\mathrm{wpn}} = 0.6$ was chosen because it represents values typical of concepts available in the literature [9]. The second value ($f_{s,\mathrm{wpn}} = 0.5$) is a perturbation case representing a low-structural mass vehicle. This example illustrates the effect of a small but significant increase in fuel mass on range. In each case $m_i = 1300$ kg, $h_0 = 10$ km, and $M_0 = 0.9$. A solid rocket booster with $I_{\mathrm{sb}} = 250$ s, $t_b = 25$ s, and $f_{\mathrm{bs}} = 0.1$ accelerates the weapon to $M_b = 3$. Dynamic pressure is varied between 40 and 100 kPa for each concept. The solid rocket motor therefore carries the weapon to an altitude and velocity that satisfies the prescribed Mach number and dynamic pressure.

Engine efficiencies, η_C and η_{KE} are set to 0.7 and 0.8 as described in Sec. II. The value $\rho_i = 900$ kg/m^3 was determined using open-literature data [24] for air-launched weapon systems and is typical of

Table 1 Baseline missile concept parameters

Parameter	Value	Parameter	Value
M_b	3.0	t_b	25 s
η_C	0.7	f_{bs}	0.1
η_{KE}	0.8	h_0	10,000 m
m_i	1300 kg	M_0	0.9
ρ_i	900 kg/m^3	ρ_f	799 kg/m^3
m_{payload}	150 kg	Υ_p	0.593
η_v	0.2	$f_{s,\mathrm{wpn}}$	0.6/0.5
C_{Do}	0.01	ρ_p	1806 kg/m^3
I_{sb}	250 s	k	1.2
f	0.0676	n	1.7

vehicles of this mass. The initial density and initial mass sets the volume and hence A_{ref} through η_v. As waverider-like characteristics have been assumed for the weapon, $n_v = 0.2$, $C_{\mathrm{Do}} = 0.01$, $k = 1.2$ and $n = 1.7$ [16]. The Mach number independence principle has been assumed, hence these parameters do not change with cruise Mach number. This assumption is supported by waverider aerodynamic data [25] which shows that lift and drag coefficients will stabilize in value above a Mach number of about 3.5.

A propellant volume fraction of 0.593 has also been calculated using solid rocket propelled air-launched booster data [24] assuming a structural mass fraction of 0.1. The liquid fuel in the weapon is Jet A and this was chosen as it is a common aviation fuel that is easily stored and handled. The scramjet system is assumed to operate at stoichiometric conditions over the airbreathing portion of the flight which implies a fuel-air ratio of 0.0676. It is argued here that an equivalence ratio of unity is the most efficient use of the captured air in the combustor.

Figures 3a and 3b summarize the results obtained for the hypersonic missile concept with 60% of the mass of the weapon devoted to structure ($f_{s,\mathrm{wpn}} = 0.6$). In Fig. 3a, the range varies between 100 and 650 km depending on dynamic pressure and cruise Mach number. High dynamic pressure has a significant effect on the range as the lower required lift coefficient allows the vehicle to cruise at a more optimal L/D setting. However, as the cruise Mach number increases, the range available drops dramatically as the fuel limitations of the vehicle are approached. This effect is also shown in Fig. 3b, which shows steadily increasing average speed for the missile concept with cruise Mach number. Above a Mach number of 8, the average speed drops significantly, due to the vehicle not having enough fuel available in the cruise phase to maintain high average speed over the mission.

Figures 3c and 3d display the results obtained from the performance model when 50% of the mass of the weapon was devoted to structure, therefore increasing the fuel capacity of the weapon. Increasing the fuel mass fraction increases the range significantly. Figure 3c illustrates this point, with maximum range at 100 kPa dynamic pressure now exceeding 1100 km and the rate of reduction in range at high cruise Mach number is much reduced compared with the previous example. Figure 3d further illustrates the benefit of increasing fuel capacity, with the average speed seen to steadily increase with cruise Mach number.

The range achieved in the cruise phase was also compared against the range calculated by the unmodified Breguet equation [16],

$$\text{range} = \frac{u_0 I_{\mathrm{sa}}}{1-\bar{g}} \left[\frac{L}{D}\right]_{\mathrm{initial}} \ell n \, \frac{W_{\mathrm{initial}}}{W_{\mathrm{final}}} \tag{16}$$

where $\bar{g} = u_0^2/(R_E + h)g$ and the L/D ratio is fixed at the value required for the start of the cruise phase. It was found that Eq. (16) predicts a range that is 6–13% lower than when using the present model where changes in L/D are taken into account.

B. Sensitivity Study

A sensitivity study has been performed using the 14 design variables that describe the baseline hypersonic missile concept. Here, each design variable is perturbed by a small amount ($\pm 1\%$) and the

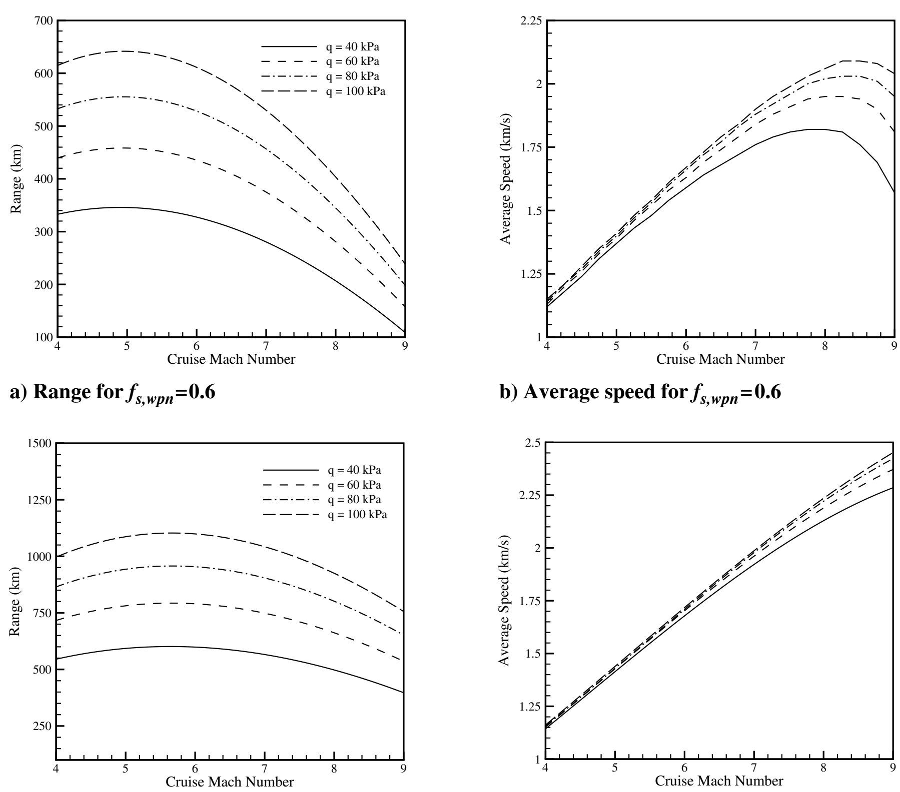

a) Range for $f_{s,wpn}$=0.6

b) Average speed for $f_{s,wpn}$=0.6

c) Range $f_{s,wpn}$=0.5

d) Average speed for $f_{s,wpn}$=0.5

Fig. 3 Hypersonic missile concept performance.

Table 2 Sensitivity study results

Parameter	Sensitivity (%)
η_{KE}	412.62
$f_{s,\mathrm{wpn}}$	−319.75
η_C	178.26
n	167.04
k	−91.62
m_i	85.39
η_v	67.31
ρ_i	−52.36
I_{sb}	19.32
z_0	5.61
M_b	−4.99
t_b	−4.99
C_{Do}	2.49
f_{bs}	−1.87

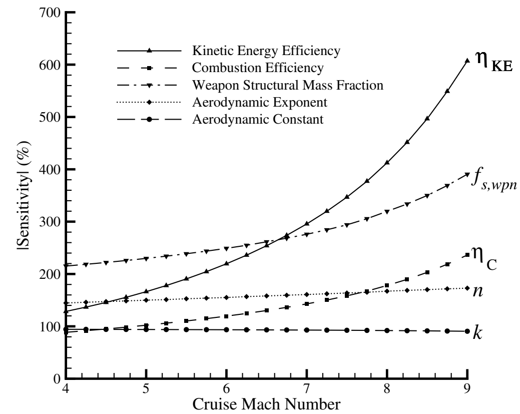

Fig. 4 Hypersonic vehicle range performance sensitivity variation with cruise Mach number ($f_{s,\mathrm{wpn}} = 0.5$ and $q = 80$ kPa).

effect on vehicle range observed. By quantifying these sensitivities, an understanding of the relative importance of each design parameter to the overall system performance is gained. This study highlights the relative importance of each design parameter and serves as a rational guide for the direction of research and development effort.

The nondimensionalized range sensitivity is defined as the normalized gradient of range to a vehicle parameter, expressed as a percentage. For example, the range sensitivity for a change in initial missile density ρ_i is,

$$\text{sensitivity (\%)} = \frac{\partial x}{\partial \rho_i}\frac{\rho_i}{R_b} \times 100 \tag{17}$$

The partial derivative in Eq. (17) is evaluated numerically by performing a perturbation analysis where input variables are systematically varied by $\pm 1\%$. The results are used to evaluate the derivative using a second order accurate numerical approximation. For the study, the baseline parameters of Table 1 (with $f_{s,\mathrm{wpn}} = 0.5$) are used with a perturbation applied to a single parameter for each computational run.

Table 2 compares the calculated sensitivities for each missile parameter and ranks them in order of magnitude. A cruise Mach number of 8 and a dynamic pressure of 80 kPa are used for the results shown in Table 2. The kinetic energy efficiency of the scramjet propulsion system is seen to have the highest sensitivity to range performance. This is an important result, as the total pressure loss associated with mixing a hydrocarbon fuel jet with supersonic air may be high and is still poorly understood. In addition, losses associated with the required flame holder and injection system may also be significant and will affect performance.

The second most sensitive parameter affecting performance is the structural mass fraction of the weapon. Combustion efficiency is seen to affect performance significantly, as do the aerodynamic parameters n and k. Again this highlights the need for accurate combustion and aerodynamic models to develop hypersonic designs. The remaining design variables, while important, do not affect the range performance as much as the combustion, geometry and aerodynamic variables.

It is also of interest to understand how range sensitivity varies with cruise Mach number. This is shown in Fig. 4, which plots the variation in range sensitivity magnitude with cruise Mach number for the five most sensitive design parameters that affect range performance in Table 2 (i.e., η_{KE}, η_C, $f_{s,\mathrm{wpn}}$, n, k).

Beginning at a cruise Mach number of 4 in Fig. 4, aerodynamics (n) and combustor losses (η_{KE}) are of equal importance, and the $f_{s,\mathrm{wpn}}$ is dominant. The structural mass fraction is directly proportional to fuel mass fraction. Also, the combustion efficiency is the least important parameter for range performance at a cruise Mach number of four. As cruise Mach number increases, the performance sensitivity is little affected by the aerodynamics over the entire flight envelope studied here. This can be partly attributed to the simplified aerodynamics model used which invokes the Mach number independence principle so that there is no change in aerodynamic coefficients with Mach number.

Combustion chamber parameters ($\eta_{\mathrm{KE}}, \eta_C$) and structural mass fraction ($f_{s,\mathrm{wpn}}$), all become increasingly more important to performance as the cruise Mach number rises. Structural (fuel storage) concerns remain dominant until a Mach number of approximately 6.7 is reached, after which, the scramjet total pressure loss (η_{KE}) becomes the most important factor affecting range performance.

Combustion efficiency does not become more important than the aerodynamics until a cruise Mach number of 7.8 is reached. While still important to range performance, combustion efficiency remains of less importance to high Mach number flight conditions than total pressure loss and structural concerns. Only well mixed fuel/air mixtures can achieve a high combustion efficiency and design constraints imply that combustion chambers must be small, thus with a short mixing length. Hence, the total pressure loss due to fuel/air mixing in a short length may be too high if a high combustion efficiency is also desired. If combustor total pressure loss dominates performance, either combustion efficiency must be sacrificed to minimize total pressure losses (thereby wasting fuel), or only a fixed fuel flow rate (or equivalence ratio) can be used, which is set by the total pressure loss of the injector design. In either case, the overall thrust may be compromised and the results displayed in Fig. 4 highlight the importance of injector design and identifying the relationship between η_{KE} and η_C for high Mach number flight and hydrocarbon fuels.

IV. Conclusion

A new hypersonic missile performance analysis model is developed and presented. The model integrates the equations of motion for a hypersonic missile over its entire mission. Models for the solid rocket booster, dual-mode scramjet propulsion system, climb thrust requirements, aerodynamics, and structural accounting are also incorporated. By integrating the equations of motion over the mission, the model is more accurate than the unmodified Breguet range equation, because changes in aerodynamic trim are accounted for during the cruise phase.

The model was used to simulate the performance of two hypersonic baseline missile concepts, whose parameters were derived from a survey of data found in the open literature but with structural mass fractions that varied by 10%. Fuel was assumed to be Jet A liquid hydrocarbon due to its handling properties, high energy per liter, and popularity in the aerospace community. For the baseline missile concept with 60% structure, maximum range occurs at a cruise Mach number of approximately 5. Average speed increases steadily until a limit is reached at a cruise Mach number between 7.5 and 8. Both range and speed performance are compromised by fuel availability for this baseline missile concept. The second baseline missile concept has a structural mass fraction of 50%, therefore allowing a greater fuel storage capacity. Higher range, average speed, and relative cruise flight time was observed.

To understand the critical issues that affect hypersonic missile performance, a sensitivity study was performed for 14 missile design parameters. At a cruise Mach number of 8, the five most sensitive design parameters relate to propulsion, structural, and aerodynamic properties of the missile. The sensitivity study was repeated over a cruise Mach number range of 4–9, where the range sensitivity was calculated for these parameters ($\eta_{KE}, \eta_C, f_{s,\mathrm{wpn}}, n, k$). It was found that at low cruise Mach numbers, structural (fuel storage) concerns dominated the range performance and combustion efficiency was of least importance. Above a Mach number of 6.7, combustor total pressure losses dominated range performance, with the structural mass fraction and combustion efficiency ranked second and third in importance. The sensitivity of range to changes in aerodynamics is almost constant over the cruise Mach numbers considered here, however, this can be partly attributed to the simplified aerodynamics model used in the performance study.

The most sensitive parameter affecting range at high Mach number is the kinetic energy efficiency of the propulsion system. It is important to note that experimental data for this parameter does not exist for supersonic combustion of hydrocarbon fuels. The effect of mixing loss on scramjet performance must be quantified and controlled, especially for hydrocarbon fuels with lower heating values and higher densities, if hypersonic missile systems are to become a reality.

Acknowledgments

This model was developed under Defense Science and Technology Organization Research Agreement No. 2004/1070598. The author would also like to thank the reviewers for their helpful suggestions that have improved the paper.

References

[1] Moses, P., Rausch, V., Nguyen, L., and Hill, J., "NASA Hypersonic Flight Demonstrators: Overview, Status and Future Plans," *Acta Astronautica*, Vol. 55, No. 3-9, Aug./Nov. 2004, pp. 619–630.

[2] Paull, A., Alesi, H., and Anderson, S., "The Hyshot Flight Program and How It Was Developed," AIAA Paper 2002-4939, Sept. 2002.

[3] Fry, R. S., "A Century of Ramjet Propulsion Technology Evolution," *Journal of Propulsion and Power*, Vol. 20, No. 1, 2004, pp. 27–58.

[4] Billig, F. S., "Supersonic Combustion Missile," *Journal of Propulsion and Power*, Vol. 11, No. 6, 1995, pp. 1139–1146.

[5] Curran, E. T., "Scramjet Engines: The First Forty Years," *Journal of Propulsion and Power*, Vol. 17, No. 6, 2001, pp. 1138–1148.

[6] Mathur, T., Gruber, M., Jackson, K., Donbar, J., and Jackson, W. D. T., "Supersonic Combustion Experiments with a Cavity-Based Fuel Injector," *Journal of Propulsion and Power*, Vol. 17, No. 6, 2001, pp. 1305–1312.

[7] Gruber, M., Donbar, J., Carter, C., and Hsu, K., "Mixing and Combustion Studies Using Cavity-Based Flameholders in a Supersonic Flow," *Journal of Propulsion and Power*, Vol. 20, No. 5, 2004, pp. 769–778.

[8] Kim, K., Baek, S., and Han, C., "Numerical Study on Supersonic Combustion with Cavity Based Fuel Injection," *International Journal of Heat and Mass Transfer*, Vol. 47, No. 2, Jan. 2004, pp. 271–286.

[9] Stuckey, R. M., and Lewis, M. J., "Hypersonic Missile Requirements and Operational Tradeoff Studies," *Journal of Spacecraft and Rockets*, Vol. 40, No. 2, 2003, pp. 292–393.

[10] Starkey, R. P., and Lewis, M. J., "Critical Design Issues for Airbreathing Hypersonic Waverider Missiles," *Journal of Spacecraft and Rockets*, Vol. 38, No. 4, 2001, pp. 510–519.

[11] Starkey, R. P., and Lewis, M. J., "Sensitivity of Hydrocarbon Combustion Modeling for Hypersonic Missile Design," *Journal of Propulsion and Power*, Vol. 19, No. 1, 2003, pp. 89–97.

[12] Starkey, R. P., "Investigation of Air-Breathing, Hypersonic Missile Configurations Within External Box Constraints," Ph.D. Thesis, University of Maryland, 2000.

[13] D. W. Riggins,, and McClinton, C. R., and Vitt, P., "Thrust Losses in Hypersonic Engines Part 1: Methodology," *Journal of Propulsion and Power*, Vol. 13, No. 2, 1997, pp. 281–287.

[14] Riggins, D., "Thrust Losses in Hypersonic Engines Part 2: Applications," *Journal of Propulsion and Power*, Vol. 13, No. 2, 1997, pp. 288–295.

[15] Masuya, G., Uemoto, T., Wakana, Y., Kudou, K., Murakami, A., and Komuro, T., "Performance Evaluation of Scramjet Combustors Using Kinetic Energy and Combustion Efficiencies," *Journal of Propulsion and Power*, Vol. 15, No. 3, 1999, pp. 401–407.

[16] Lewis, M. J., "Significance of Fuel Selection for Hypersonic Vehicle Range," *Journal of Propulsion and Power*, Vol. 17, No. 6, 2001, pp. 1214–1221.

[17] Bilimoria, K., and Schmidt, D., "Integrated Development of the Equations of Motion for Elastic Hypersonic Flight Vehicles," *Journal of Guidance, Control, and Dynamics*, Vol. 18, No. 1, 1995, pp. 73–81.

[18] Miele, A., *Flight Mechanics, Volume 1, Theory of Flight Paths*, Addison–Wesley Publishing Company, USA, 1962.

[19] Curran, E., Leingang, J., Carreiro, L., and Petters, D., "Review of Kinetic Energy Methods in High Speed Engine Cycle Analysis," *10th International Symposium on Air Breathing Engines*, AIAA, Reston, VA, 1992.

[20] Kerrebrock, J., "Some Readily Quantifiable Aspects of Scramjet Engine Performance," *Journal of Propulsion and Power*, Vol. 8, No. 5, 1992, pp. 1116–1122.

[21] Raymer, D., *Aircraft Design: A Conceptual Approach*, 3rd ed., AIAA Education Series, AIAA, Reston, VA, 1999.

[22] *U.S. Standard Atmosphere, 1976*, U.S. Government Printing Office, Washington, DC, 1976.

[23] Carmichael, R., "1976 U.S. Standard Atmosphere," *Public Domain Aeronautical Software* [online database].

[24] *Aerospace Source Book*, Aviation Week and Space Technology, Washington, D.C., 2002.

[25] Cockrell, C., and Huebner, L., "Aerodynamic Characteristics of Two Waverider-Derived Hypersonic Cruise Configurations," NASA TP-3559, 1996.

P. Weinacht
Associate Editor